



A99-31508

AIAA 99-2842

MHD Slipstream Accelerator Investigation in  
the RPI Hypersonic Shock Tunnel

J.M. Kerl , L.N. Myrabo, H.T. Nagamatsu, M.A.S. Minucci,  
and E.D. Meloney

Rensselaer Polytechnic Institute  
Troy, NY

**35th AIAA/ASME/SAE/ASEE Joint Propulsion  
Conference and Exhibit  
20-24 June 1999  
Los Angeles, California**

## MHD SLIPSTREAM ACCELERATOR INVESTIGATION IN THE RPI HYPERSONIC SHOCK TUNNEL

J.M. Kerl,\* L.N. Myrabo,<sup>†</sup> H.T. Nagamatsu,<sup>‡</sup> M.A.S. Minucci,<sup>§</sup> E.D. Meloney\*  
 Rensselaer Polytechnic Institute  
 Troy, NY 12180

### Abstract

The feasibility of a hypersonic Magneto hydrodynamic (MHD) engine was investigated in the RPI Hypersonic Shock Tunnel (HST) by decelerating the flow in a MHD channel. The effect of power extraction was observed by measuring current and noting changes in shock position through Schlieren photography. The MHD combined cycled engine proposed that the application of crossed electric and magnetic fields to the plasma, created by the high temperature compressed gas, would accelerate or decelerate by the Lorentz body force.<sup>1</sup> The creation of this force would also change the pressures in the desired region and therefore the shock positions. The axisymmetric 7-in Plexiglas model was fitted with 24 MHD channels, three MHD channel impact pressure probes, and internally, two 4-in Bitter solenoid electromagnets. The model was installed and tested in the RPI 24-in HST and integrated to the 50-kJ, 10-kV Maxwell Pulsed Power Supply (PPS). The same model contour was previously investigated in the RPI HST to obtain the flow field near the cowl,<sup>2,3</sup> however, no MHD studies on this model were conducted. The plasma characteristics were determined by extracting power from MHD channels and observations were made of the flow behavior.

### Introduction

The MHD engine was originally designed as a second stage investigation of the Lightcraft.<sup>1,4</sup> The motivation for the present study is based on the limitations that rocket and jet propulsion systems exhibit in the upper atmosphere. The limit comes

basically in the amount of fuel that the craft can carry. At an altitude where air is sparse and the Lightcraft's ground based laser propulsion system would be insufficient in providing an adequate amount of thrust, the MHD engine would be in its altitude regime cruising at Mach 8 with its airbreathing, near fuel-less design. The MHD accelerator would be used in conjunction with an Air Spike,<sup>5</sup> modifying the bow shock wave to reduce drag and heating while creating external plasma in the shock layer.

The primary objective of this investigation was to determine the feasibility of the MHD engine by attempting to decelerate the flow and extract power or essentially change the kinetic energy of the flow into electrical potential energy. This model was incapable of accelerating the flow for two reasons: First it was determined that a high voltage would be necessary for the production of the electric field since the naturally occurring conductivity was low. Also this model was equipped with two Bitter solenoids requiring a high voltage power supply to produce a strong magnetic field and the originally designed electrodes would not withstand such a high power. Currently, researchers at RPI are testing a 2D wedge model used to attempt flow acceleration utilizing permanent magnets instead of electromagnets. This model is essentially one of the 24 MHD channels of this axisymmetric model. The 2D-wedge experiment incorporates 1/4-in. copper electrodes to withstand high current from the PPS.

### Experimental Apparatus

The MHD model consisted of a Plexiglas 7-in diameter complex contour scaled from the Lightcraft,<sup>3</sup> 24 electrodes, and two Bitter solenoid magnets. Figure 1 shows a cross sectional view of the MHD model and all of its components. The compression surface inlet geometry had been previously designed and details of the contour can be found in Ref. 6. The electromagnets, called Bitter solenoids, were designed to produce a 10 T field at the centerline and a 0.15 T field at the radial location in the MHD channel. Four, model 111A22, PCB quartz pressure transducers were used. Three were located 120 degrees apart to measure impact pressure through the MHD channels and one was used as a pitot probe. All pressure transducers were recalibrated in the RPI Low Pressure Shock Tube after testing to insure that no damage was done due to

\* Graduate Student, AIAA Student Member

<sup>†</sup> Associate Professor of Aeronautical Engineering, AIAA Member

<sup>‡</sup> Active Professor Emeritus of Aeronautical Engineering, AIAA Fellow

<sup>§</sup> Visiting Aeronautical Engineer, AIAA Member

Copyright © 1999 by the American Institute of Aeronautics and Astronautics, Inc. All rights reserved.

the magnetic fields. The axisymmetric model, designed and fabricated at RPI, was installed in the RPI HST test section and integrated with the Maxwell Capacitor PPS. Figure 2 shows the model installed in the test section. A simple co-axial cable was constructed to integrate the Maxwell capacitor bank, the model and the test section. A 2-in copper pipe was used as the outside conductor, a welding cable as the inner conductor and 1-in thick nylon discs were used as spacers for the construction of the co-axial cable. Inside the test section, another coaxial power line using 1.5-in copper pipes and the same welding cable was assembled and a special vacuum feed through plate was made, cf. Fig 2. The two Bitter electromagnets and the Maxwell Capacitor PPS were used to produce the magnetic field and were donated by US Army.

The original model was equipped with iron core laminates between the two electromagnets which were machined to fit the model contour. They were removed and replaced with a Plexiglas piece for reasons stated later.

Attempting to extract power from all 24 MHD channels proved to provide indiscriminate and inaccurate results, and tests were modified to extract power from just one MHD channel.

#### RPI 24-in. Hypersonic Shock Tunnel

The RPI 24-in HST, cf. Fig 4, hosted all MHD slipstream interaction tests. The equilibrium interface mode of operation was used to obtain higher enthalpies, producing more electrical conductivity than the tailored mode of operation.<sup>7</sup> Enthalpies can be up to 6.5 MJ/kg when run in the equilibrium interface mode. All runs were conducted at Mach 8, the lowest Mach number available at the RPI HST that enables the most test gas to enter the test section, allowing for more density, while still keeping a high temperature, high speed flow. Figure 5 shows the shock tunnel instrumentation and setup. The HST has a 15-ft driver with a 4-in internal diameter. Room temperature helium was used as the driver gas at a maximum pressure of 2000 psig. The double diaphragm section was filled with argon to limit contact surface mixing. The 55-ft long, 4-in internal diameter, driven section was evacuated and loaded with dry air as the test gas to 25 torr. A thin (0.015 in) aluminum diaphragm separated the driven tube from the nozzle and test section. The 24-in exit diameter brass nozzle exited into the 200 ft<sup>3</sup> test section/dump tank, which was evacuated to 70  $\mu$ Hg on average. A detailed explanation of the Shock Tunnel can be found in Ref. 8.

#### Results and Discussion

Tests of the electromagnets were conducted to characterize the magnetic field within the MHD

passages. These tests were performed outside of the tunnel test section for simplicity. Several minor problems were detected during these tests when the output power of the Maxwell bank was varied from 10 to 50%. Such problems encompassed arcing in the electrical contacts and insufficient sampling rate in the data acquisition system. Improving the electrical insulation of the conductors as well as removing the iron core laminates solved the arcing problem. This was justified by a very small loss in the magnetic field strength at the location of interest. Consulting with an independent research engineer from Army Research Lab<sup>7</sup> provided insight to the cause of the small increase in the magnetic field that the iron laminates provided. Iron core laminates are useful for low currents and low field requirement, but application of large currents cause the metal laminates to saturate and there would be no significant increase in the magnetic field. In this situation, the coils are in a bucking configuration where the field at the centerline is approximately 10 T. The iron core laminates saturate at 1-2T and therefore provided no increase in the field at all until the radial position where the field is below 1-2 T. Since the field drops off rapidly as a function of radial position, only the very ends of the laminates were helping increase the field. Test concluded that the field with and without the laminates did not differ drastically, cf. Fig 6. Figure 6 shows the peak radial field intensity as a function of the coil current for various configurations.

Luminosity photographs were taken both with and without a pulse of the electromagnets. Results from runs at an average free stream Mach number of 7.6, a stagnation temperature of 4,050 K, are presented in Fig. 7. A photograph was also taken of a pulsing of the coils without a shock tunnel run to determine that no luminosity was present from the pulsing of the coils. It is clear from Fig. 7 that the pulsing of the coils induces a force, which slows the flow down, making the open shutter luminosity photograph much brighter. During the open shutter luminosity photographs a 50  $\Omega$  resistor was connected in series to the 24 electrodes, which were connected in parallel in much the same way performed by Nagamatsu et al.<sup>8</sup> It is important to point out that no external electrical potential was applied to the electrode fins; the flow deceleration was generated by the conducting air plasma flowing between the electrodes and by the fact that all the negative electrodes were electrically grounded.

Current was also extracted during the luminosity photographs, but the data was unreliable. The configuration was changed to measure across one set of electrode fins instead of across all 24. This eliminated any probability of a current loop within the 24 fins. A current loop was largely feasible due to the unsteady, unstable nature of a weakly ionized gas,

providing different emf values for different fin locations.

Another result of equal importance was to measure flow pressure in the MHD channels. This is important to obtain parameters of the flow electrical conductivity. Impact pressure probes, installed in three MHD passages, 120 degrees apart, yielded an average pressure of 0.58 psi. The average free stream pitot pressure was 2.0 psi. In addition to the impact pressure probes, Schlieren photographs of the flow structure near the passage inlets were taken to determine the effect of the magnetic field and energy extraction, from the slipstream, on the bow shock wave. Figure 8 shows Schlieren photograph comparison of a flow with and without a pulsing of the magnets. The bend in the bow shock wave indicates a definite deceleration of the flow.

For the 0.15 T magnetic field applied, the current across one of the channels was measured for an external resistance varying from 106 k $\Omega$  to .47  $\Omega$ , cf. Fig 9. The expected open circuit voltage was determined by the following equation,

$$V = \frac{UBL}{10^8}$$

where U is velocity in cm/sec, B is magnetic field in Gauss, and L is the electrode gap in cm. The expected voltage was determined to be 770 mV. Figure 10 shows the extracted voltage verses the external resistance. Clearly there are different regimes in which the current extraction behaves. There appears to be a threshold current of 1 A after which the power extracted behaves as a real generator. Figure 10 shows the power, calculated from the external current and extracted voltage. It is clear that this MHD flow deceleration, which should act as a power generator, only behaves with half of it's potential. This is indicated by the power curve, in that a generator should be a bell curve, and this 'MHD Generator' is clearly not a bell curve; however, if data is separated to include only point were a current above 1 A was yielded the behavior is different. Figure 11 and Fig. 12 are the voltage and power curves for data above 1 A, respectively.

### Conclusion

An axisymmetric hypersonic MHD engine was investigated, specifically it's feasibility. Tests were performed at a freestream Mach number of 7.6 with 4050 K reservoir temperature. The investigation was successful in that the proof that the flow was disturbed and decelerated. Changes in the luminosity and the bow shock wave were apparent. Power was extracted even though only a weakly ionized gas was present. As a generator, this MHD generator only provided enough power to obtain the first part of the power bell curve.

Future suggestions include trying to increase the electrical conductivity of the flow, investigated the 2D wedge "blown up channel", perform CFD analysis in the channel.

### Acknowledgements

The authors wish to acknowledge the NASA Marshall Space Flight Center for their support of this study. Special thanks to the US Army and PCB Piezotronics, who donated equipment and the IMS machine shop who was responsible for model construction. The authors would like to thank A. Zielinski, D.G. Messitt, C.A. Andrade, A.D. Panetta, C. Vannier, W. Meilke, and C. McKeown for their assistance.

### References

1. Moder, JP, Myrabo, LN, and Kaminski, DA, "Analysis and Design of Ultrahigh Temperature Hydrogen Fueled MHD Generator," *Journal of Propulsion and Power*, v 9, n 5, Sept-Oct, 1993, pp739-748.
2. Jones, RA, Myrabo, LN, Nagamatsu, HT, and Minucci, MAS, "Experimental Investigation of an Axisymmetric Hypersonic Scramjet Inlet for Laser Propulsion," *Journal of Propulsions and Power*, v 8, Nov, 1992, pp1231-38
3. Messitt, DG, "Computational and Experimental Investigation of 2-D Scramjet Inlets and Hypersonic Flow Over a Sharp Flat Plate" PhD Thesis Dissertation, Rensselaer Polytechnic Institute, Troy, NY, May, 1999.
4. Myrabo and Raizer, "Laser Induced Air Spike for Advanced Trans-atmospheric Vehicles," AIAA-9492451, June, 1994
5. Diaz, E, Toro, PGP, Myrabo, LN, Nagamatsu, HT, and Messitt, DG, "Experimental Pressure Survey of the Hypersonic Air Spike Inlet at Mach 10," AIAA 96-3143, June 1996.
6. Kerl, JM "An Experimental Investigation of a Magnetohydrodynamic Engine," Master Thesis, Rensselaer Polytechnic Institute, May, 1999.
7. Minucci, MAS and Nagamatsu, HT, "Hypersonic Shock Tunnel Testing at an Equilibrium Interface Condition of 4100 K," *Journal of Thermophysics and Heat Transfer*, vol. 7, 1993, pp. 251-260.
8. Minucci, MAS, "An Experimental Investigation of a 2-D Scramjet Inlet at Flow Mach Numbers of 8 to 25 and Stagnation Temperatures of 800 to 4100 K," PhD Thesis Dissertation, Rensselaer Polytechnic Institute, Aug. 1991.

9. Personal Conversations, Alex Zielinski, Army Research Laboratories.
10. Nagamatsu, H.T. and Sheer, R.E., Jr. "Magnetohydrodynamic Results for Highly Dissociated and Ionized Air Plasma Produced by Hypersonic Shock Waves." General Electric Research Laboratory Report No. 61-RL-2602C, Schenectady, NY, Jan. 1961.

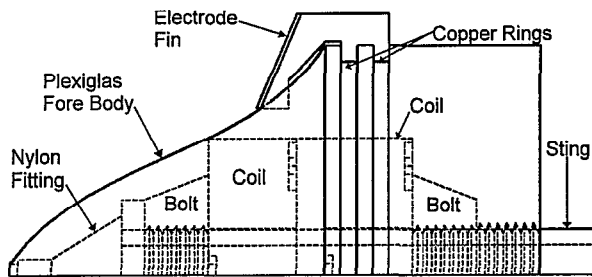


Fig. 1 MHD Model Cross Sectional View

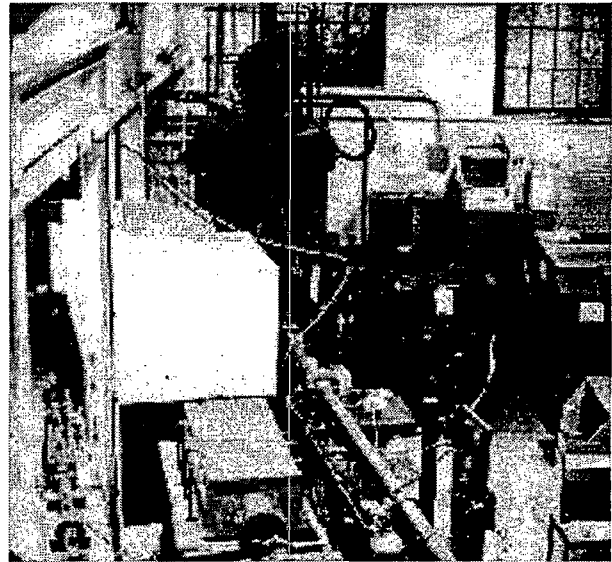


Fig. 4 RPI Hypersonic Shock Tunnel

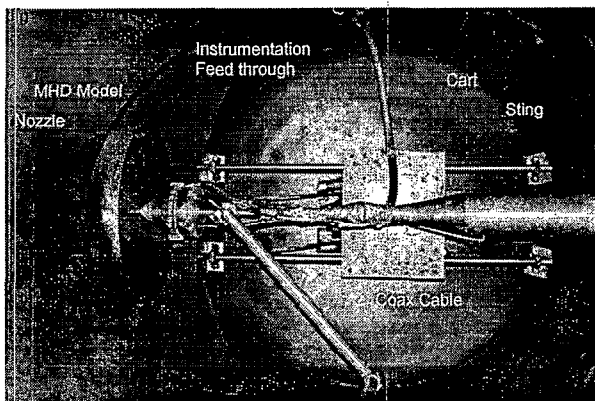


Fig. 2 MHD Model Installed in the Test Section

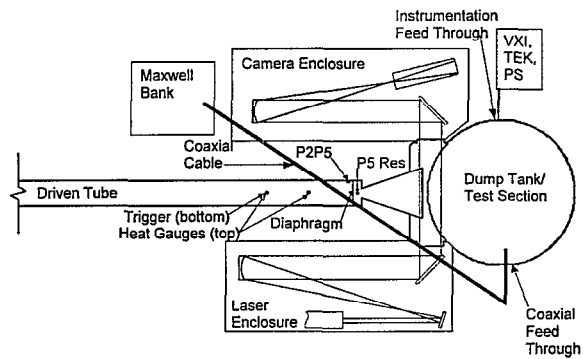


Fig. 5 RPI HST Instrumentation Diagram

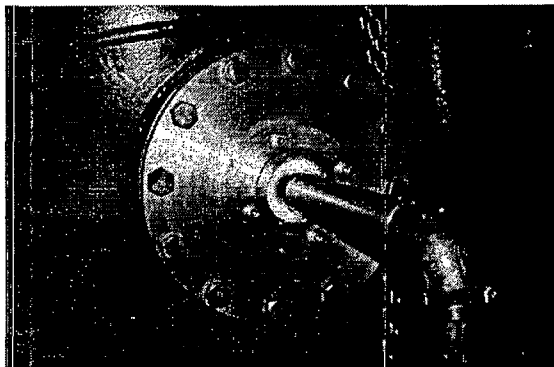


Fig. 3 Co-axial Cable and Vacuum Feed Through Plate Into the Test Section

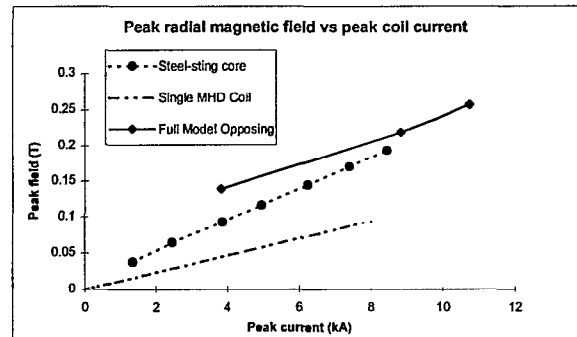


Fig. 6 Peak Radial Magnetic Fields in Various Configurations

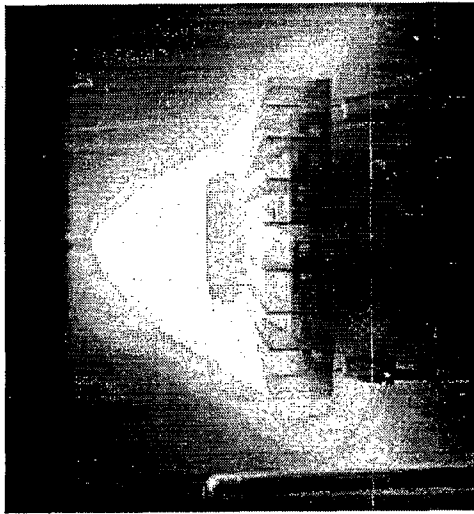


Fig. 7A Luminosity Photograph Without Pulsing Magnets

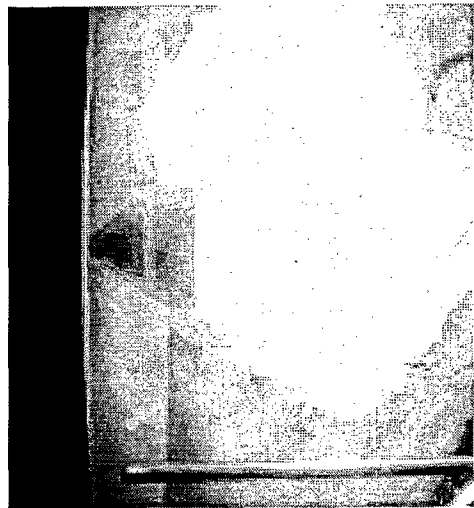


Fig. 7B Luminosity Photograph While Pulsing Magnets



Fig. 8 Schlieren Photograph Comparison between a Run Without and With Pulsing of the Coils

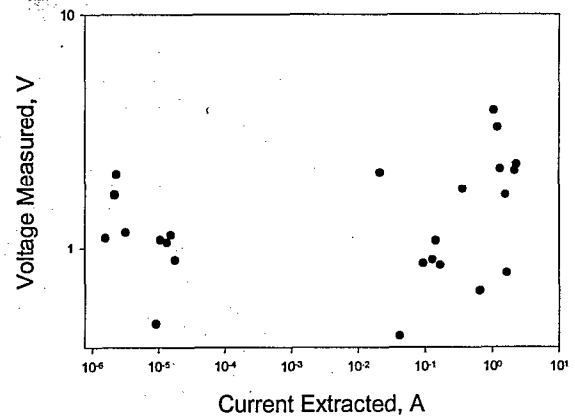


Fig. 9 Current Extracted vs. Voltage Measured

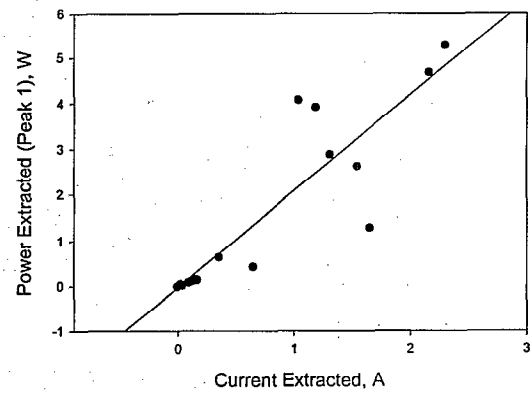


Fig. 10 Power Curve for the MHD Generator

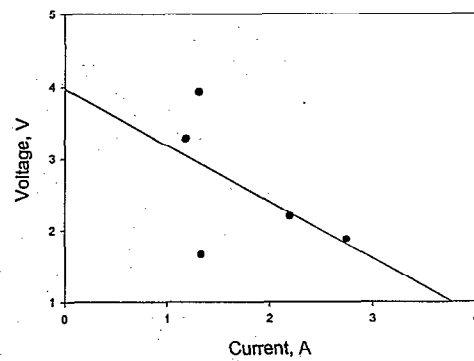


Fig. 11 Current Extracted versus Voltage Measured, Greater Than 1 A

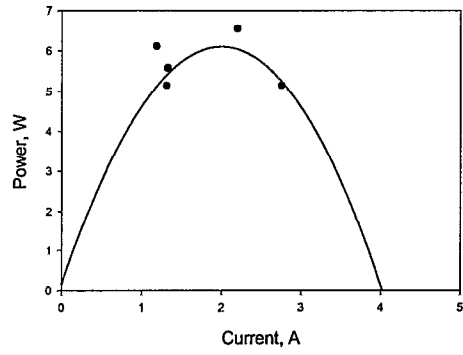


Fig. 12 Power Curve for the MHD Generator, Greater Than 1 A